

SIMULTANEOUS TOPOGRAPHY OPTIMIZATION OF A VEHICLE HULL AND TOPOLOGY OPTIMIZATION OF THE ASSEMBLY INTERFACE FOR BLAST MITIGATION

Huade Tan
John Goetz

Andrés Tovar, PhD
John E. Renaud, PhD

Department of Mechanical and Aerospace Engineering
The University of Notre Dame
Notre Dame, IN

ABSTRACT

Structural optimization efforts for blast mitigation seek to counteract the damaging effects of an impulsive threat on critical components of vehicles and to protect the lives of the crew and occupants. The objective of this investigation is to develop a novel optimization tool that simultaneously accounts for both energy dissipating properties of a shaped hull and the assembly constraints of such a component to the vehicle system. The resulting hull design is shown to reduce the blast loading imparted on the vehicle structure. Component attachment locations are shown to influence the major deformation modes of the target and the final hull design.

INTRODUCTION

Gross vehicle acceleration, often measured in peak and sustained g's, is of interest in the vehicle level blast mitigation problem. Unlike frontal crash events, the acceleration of the vehicle achieved during a blast event translates to vertical loads exerted on the pelvis and compression of the spinal cord, resulting in injuries and fatalities in the field [1]. The key to mitigating such loading events is the reduction of the fluid structure coupling between the blast and the vehicle, and the mechanical isolation of the occupant from the vehicle [2, 3].

When armor systems are mounted to existing vehicle platforms to mitigate penetration or blast induced occupant injuries, the dynamics of the vehicle itself may be altered by the added weight and the positioning of such components. Vehicle level design requirements drive both the design of the armor component and the structure to which the armor attaches. The Hybrid Cellular Automata (HCA) based design algorithm developed in this work seeks to solve

both these problems simultaneously. The need to solve both of these problems in parallel is shown to be driven by the nature of the blast mitigation problem and the dynamic response of the vehicle system.

The effectiveness of armor systems in both blast and penetration events is highly dependent upon the structure to which the armor system is mounted [4, 5]. Considerable stresses are transferred between the armor system and the vehicle during a blast event. Such stresses are a significant factor in the dynamic response of the target structure as well as the failure mode of the armor component. As is shown in this effort, the considerations of both the armor and mating structures deal with the same coupled design problem. In the following investigation, the topology optimization approach proposed by Buhl [6] is used to develop concept designs of both the hull and mounting systems.

Blast mitigation efforts have historically taken two directions. Methods of energy absorption, as presented in [7-9] focus on the armor component and

seek to transform the blast energy imparted on a target in the form of plastic strain energy. Methods of energy dissipation, as presented in [3, 10-12] evaluate the effects of deflecting the blast energy imparted on a target by channeling high pressure blast products away from the target structure. While both methods are actively being pursued in research, the energy deflection method has subsequently been proven in industry applications. We seek to evaluate the fluid structure problem while implementing geometric constraints for the design of mounting such components to the vehicle system.

Fluid structure interaction mitigation design methods have previously been implemented to simulate the blast event and to minimize the corresponding load on the target structure. Nodal update algorithms consistent with the blast HCA methodology described in [3] have been shown to develop novel shapes that yield significant impulse and peak pressure reductions over standard target geometries. Such mitigation behaviors have been shown to reduce the blast loading generated from both surface and shallow buried detonation events. Due to the discrete nature of the topology design method derived by Buhl et al. [6], a similarly discrete method such as blast HCA is appropriate for handling the algorithmic coupling of these structural interaction problems.

A formulation is derived, taking from Buhl's method, to obtain the ideal shape and mounting locations of a thin wall target plate mounted over a vehicle substructure. As described in [6], the structural topology design problem is highly dependent upon the boundary conditions of the finite element model. It is expected that the same effects will be exhibited in the application to the blast mitigation problem.

For the purpose of minimizing fluid structure interaction between the blast wave and target structure, the deformation of the target structure is minimized. Hanssen and Pytleski et al. [2, 11] highlight the effect of dishing in magnifying the blast energy transferred to a target structure. In order to minimize this energy transfer mechanism, we seek to minimize the structural deformation of the structure during the blast event.

NUMERICAL FORMULATION

A reduced vehicle model is developed for the simulation of a surface and shallow buried blast event using the baseline geometry of the Defense Research and Development Canada (DRDC) plate described by Williams et al. [13]. The reference DRDC plate geometry is scaled down and imbedded in a Multi

Material Arbitrary Lagrange Eulerian (MMALE) model where the detonation event takes place. The response of this reduced vehicle model to the MMALE blast load is taken to be the objective measurement for blast mitigation in the design objective formulation.

The MMALE fluid structure interaction finite element formulation developed by Souli et al. [14] is a numerical method designed for solving large deformation problems that occur at a very fine timescale. The finite element mesh is allowed to move independently from the flow of the material. Each element may contain a mixture of materials. The ALE domain is a global reference frame on top of the spatial and material domains, which correspond to the Eulerian and Lagrangian domains respectively. As the Lagrange domain moves in time, the state variables are mapped back to the Eulerian mesh locations during an advection step. Either the Young or the volume of fluid (VOF) method is used to track an interface in elements containing more than one material. The key interest of the MMALE finite element method is its ability to maintain quality mesh geometry independent of material geometry.

The formulation of a free field detonation of high explosive in ALE was described by Souli et al. [14]. The MMALE formulation is well suited for the simulation of such events because of its convenient method of treating moving boundaries, free surfaces, and material interfaces. Air is modeled with an ALE mesh using a hydrodynamic material model. ALE requires the definition of an equation of state (EOS), density, pressure cut-off, and viscosity coefficient of all fluid materials. For air, the viscosity and pressure cut-off are zero since pressure cannot be negative and viscosity can be considered negligible within the time scale of the problem.

The ideal gas law is used as the equation of state for air, in which the pressure is defined as

$$p = C_0 + C_1\mu + C_2\mu^2 + C_3\mu^3 + E(C_4 + C_5\mu + C_6\mu^2), \quad (1)$$

where p is the pressure, $\mu = \frac{\rho}{\rho_0} - 1$ and $C_1 \rightarrow C_6$ are fitting coefficients. Assuming properties of an ideal gas, coefficients $(C_0, C_1, C_2, C_3, C_6)$ become 0 and C_4, C_5 become $\gamma - 1$, reducing Equation (1) to

$$p = (\gamma - 1) \frac{\rho}{\rho_0} E, \quad (2)$$

Simultaneous Topography Optimization of a Vehicle Hull and Topology Optimization of the Assembly Interface For Blast Mitigation, Tan, et al.

where ρ and ρ_0 are the current and initial densities of air, E is the specific internal energy and γ is the ratio of specific heats (typically 1.4 for air). An internal energy of 2.5 bar is assigned to air such that the ambient pressure is 1 bar. The ALE domain is sealed with fixed boundary constraints at the exterior surfaces to preserve total energy of the system and to prevent air from leaking out of the domain.

For simulating the explosive charge and its detonation products, the density, EOS, detonation velocity and Chapman Jouguet pressure must be defined. The Jones-Wilkins-Lee (JWL) EOS was selected to model high explosives for its simplicity and widely accepted usage. The JWL EOS starts from its isentropic form as

$$p_s = Ae^{-R_1 V} + Be^{-R_2 V} + CV^{-(\omega+1)}, \quad (3)$$

where p is the pressure of the explosive product, and the subscript s denotes the reference to isentropic compression or expansion. The standard form of the JWL EOS is given by

$$p_{JWL}(V, E) = A \left(1 - \frac{\omega}{R_1} V\right) e^{-R_1 V} + B \left(1 - \frac{\omega}{R_2 V} e^{-R_2 V}\right) + \frac{\omega}{V} E, \quad (4)$$

where A, B, R_1, R_2 and ω are explosive dependent constants, p is the pressure and V is the relative volume. R_1 is chosen about four times larger than R_2 so that at high pressures the first term dominates, at intermediate pressures the second term, and at low pressures the third term. The first term in the JWL EOS is the high pressure term and dominates for V close to 1. The second term dominates for V close to 2. For $V \rightarrow \infty$, the JWL EOS reduces to the third term. Note that the last term in the polytropic EOS for air is equal to the third term in the JWL EOS. With $\omega = \gamma - 1$, the JWL and ideal gas pressures match asymptotically for large volumes. JWL EOS constants for TNT and C₄ are given in table 1.

Parameter (units)	C4	TNT
A (Mbar)	5.981	3.712
B (Mbar)	0.138	0.032
R_1	4.5	4.15
R_2	1.5	0.95
E (Mbar)	0.087	0.070
ω	0.32	0.3
v_d (cm/ μ s)	0.804	0.693
ρ (g/ cm^3)	1.601	1.590

Table 1: Summary of C4 and TNT equation of state parameters.

Soil is modeled using material number five in LS-DYNA (MAT_SOIL_AND_FOAM) [15], which acts as a fluid with a simple pressure dependent flow rule.

$$\phi_s = \frac{1}{2} s_{ij} s_{ij} - (a_0 + a_1 p + a_2 p^2), \quad (5)$$

where ϕ_s is the flow stress of the material, a_0, a_1, a_2 are user defined yield function constants, s_{ij} are the components of the deviatoric stress tensor, and p is the hydrostatic pressure. The density ρ , shear modulus G , and bulk modulus of the material are also defined in this model. For the purposes of this study, the material properties of dry sand as defined by Neuberger et al. [16] were used to simulate the soil media.

The MMALE simulation of an explosion is carried out in two stages. Before the detonation, $t < t_{det}$, the explosive charge, is treated as a solid with density $\rho = \rho_0$. The geometry of the explosive charge may be specified by the user in any FE preprocessor. At time $t = t_{det}$, the detonation of the charge occurs at a user defined location (must be within the volume of the charge).

The first stage of an MMALE blast simulation is defined by the solution of the detonation event. The detonation process of an explosive is modeled by a material specific detonation velocity v_d , where the material ahead of the detonation front is still treated as a solid while the material behind the detonation front is treated as a high pressure gas defined by equation (4). During this detonation stage, p_{JWL} is dominated by the first term and the charge is converted into a high pressure gas with the same mass and approximately the same volume as the initial solid.

The second stage of an MMALE blast simulation is defined by the solution of the high pressure gas interacting with the environment: generating shock waves in the media surrounding the charge. In the MMALE formulation, this interaction process is carried out by the standard advection methods proposed by Souli et al. [14] where user defined environments such as air, soil or structural boundaries are specified using any FE preprocessing software. This stage of the blast event is of particular interest in the blast mitigation problem. The dynamic interaction of the shock waves generated by the expansion of the blast product is the primary mechanism by which vehicle structures are loaded during the blast event.

The baseline numerical model consists of one quarter of a steel target plate, modeled after the Williams et al. DRDC plate geometry [13], is situated directly above a

Simultaneous Topography Optimization of a Vehicle Hull and Topology Optimization of the Assembly Interface For Blast Mitigation, Tan, et al.

square explosive charge. One quarter of the target and ALE domain is modeled, using necessary reflecting boundary conditions, in order to reduce the overall computational cost of each finite element run. During the simulation, the detonation product is reflected from the soil and directed toward the target. The interaction and reflection of the blast wave with the target plate determines the pressure load and response of the target structure. It is this fluid structure interaction and pressure load which we seek to minimize in order to mitigate the effects of blast loading on the vehicle occupants.

The design domain is assumed to be the entire area of the target surface. Nodal locations of the reference surface are taken to be the set of design variables in the topography design problem. The blast HCA topography optimization scheme continually updates the nodal locations of the target to arrive at a convex energy deflecting structure based on tested fluid structure interaction properties. A schematic of the fluid structure interaction design domain is given in figure 1.

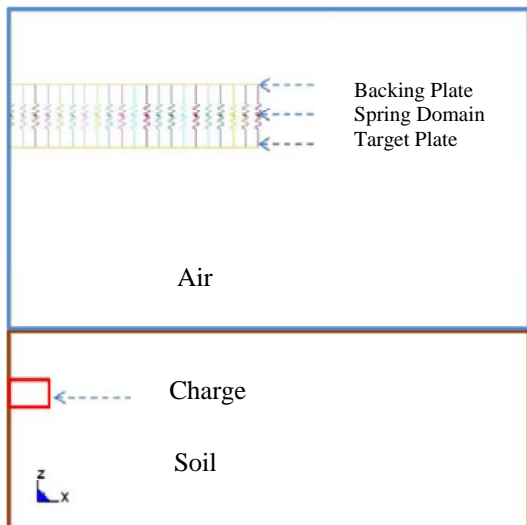


Figure 1: Schematic of a shallow buried detonation geometry showing only one half of the symmetric detonation profile.

A secondary design domain is defined along the outer perimeter of the reduced DRDC plate as the range of possible attachment points [6]. This second design domain is consistent in resolution with the nodal HCA design domain but does not occupy the entire area of the target plate. The region of highest blast loading was excluded intentionally in order to induce a geometric constraint on the problem as would be expected of a vehicle level application. The vehicle

Simultaneous Topography Optimization of a Vehicle Hull and Topology Optimization of the Assembly Interface For Blast Mitigation, Tan, et al.

designer would select the design domain and baseline geometries of such a simulation based on platform requirements. A schematic of this model problem is depicted in figures 2 and 3.

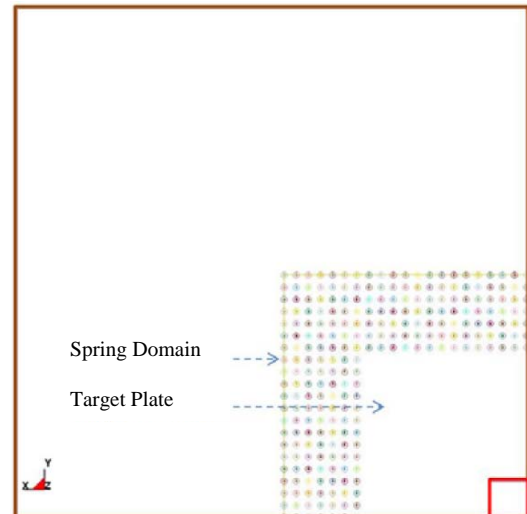


Figure 2: Schematic of the separate topography and support design domains adopted from the Williams DRDC plate geometry for the simultaneous design evaluation. Only one quarter of the plate geometry is depicted in the above diagram.

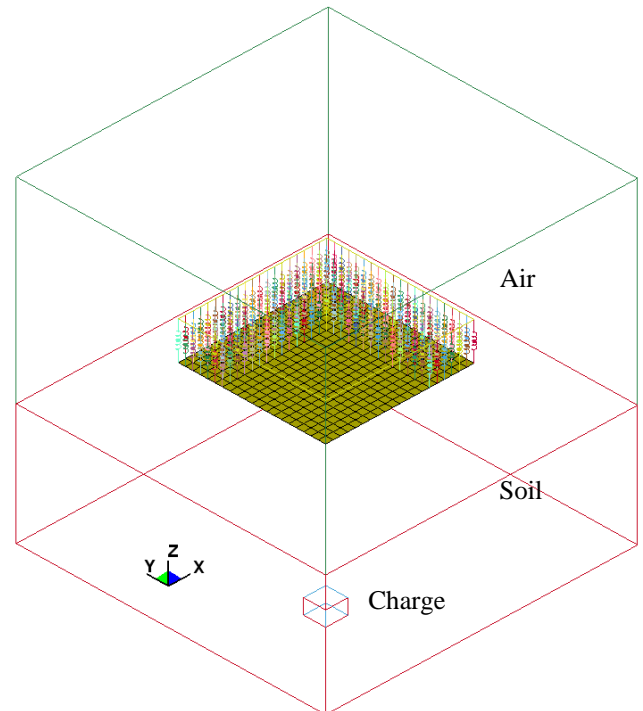


Figure 3: Isometric view of the full MMALE domain and target geometry. The ballast structure is not depicted in order to show the support design domain.

HCA DESIGN FORMULATION

The hybrid cellular automata algorithm was first formulated for the purpose of solving the minimum compliance problem by Tovar et al. [17, 18]. The application of HCA to the design of supports is therefore very similar to the original algorithm formulation. The blast HCA topography optimization formulation was introduced by Tan et al. [3], where a nodal update cellular formulation was developed to design the shape of a target structure for minimum fluid structure interaction.

Two sets of design variables, z_i and s_i , exist in the coupled optimization problem. The design variable z_i defines the characteristic shape of the design while the design variable s_i defines the stiffness of each spring in the support design domain by

$$k_f = s^P k_0, \quad s_{min} < s \leq 1, \quad (6)$$

where k_f is the spring constant of each nodal support location, P is a stiffness penalty factor and k_0 is the maximum spring constant defined in this investigation as the modulus of steel times the length of the spring.

Support locations were modeled using linear elastic discrete spring elements in LS-DYNA of uniform length and variable stiffness. These springs connect the target surface with a ballasted vehicle model as a rough approximation of a vehicle substructure interface. In this investigation, the backing plate is ballasted by simply setting a large density for the backing plate material. The coupled fluid structure interaction problem is expressed as a minimization of the dynamic response of the design domain subject to certain geometric and design limits as follows:

$$\begin{aligned} \min_{z,k} \max_t \quad & a(z, k, t) + I(z, k) \\ \text{subject to} \quad & S^T f \leq S^* \\ & 0 < z_{min} \leq z \leq 1 \\ & 0 < s_{min} \leq s \leq 1 \end{aligned} \quad (7)$$

where $a(z, k, t)$ and $I(z, k)$ are the nodal responses of the target domain obtained in LS-DYNA. The variable a is the nodal z acceleration obtained from the LS-DYNA nodout file and I is calculated as

$$I(t) = \sum_t a_i(t). \quad (8)$$

From the monotonic inverse relationship between target convexity and cabin penetration presented in [3],

Simultaneous Topography Optimization of a Vehicle Hull and Topology Optimization of the Assembly Interface For Blast Mitigation, Tan, et al.

the objective of the shape optimization formulation is taken to be

$$e_i = (I_i - a_i) \cdot \delta_{max} - z_i, \quad (9)$$

where the state variables of peak acceleration (a_i) and impulse (I_i) are the normalized values obtained from the finite element analysis at each node. Using a direct proportional control method, the continuous local blast HCA update is

$$\Delta z_i = \frac{e_i(k)}{z_i(k)}, \quad (10)$$

where $e_i(k)$ is the iterative error signal obtained from Equation (9) and the iterative update of the design variable $z_i(k+1)$ is expressed as

$$z_i(k+1) = \bar{z}_i(k) + d\bar{z}_i(k), \quad (11)$$

where \bar{z}_i and $d\bar{z}_i$ are the neighborhood average values obtained from the cellular automata definition

$$\bar{z}_i(t) = \frac{z_i(t) + \sum_j^N z_j(t)}{N+1}. \quad (12)$$

As defined in Equations (2) and (1), the minimum compliance problem is essentially a maximum stiffness problem which minimizes the total number of supports. The minimum compliance problem may be written as a local design update as follows:

$$\begin{aligned} \min_s \quad & |U^* - \bar{U}_i(s_i)| \\ \text{subject to} \quad & 0 < s_{min} \leq 1, \end{aligned} \quad (13)$$

where U^* is the local strain energy target and \bar{U}_i is the average strain energy in a local CA neighborhood. The strain energy of each spring U_i is output in the elout file of each LS-DYNA run. The average strain energy \bar{U}_i is obtained from

$$\bar{U}_i(t) = \frac{U_i(t) + \sum_j^N U_j(t)}{N+1}, \quad (14)$$

where the sub-index j refers to the neighboring cells in the cellular automata environment. Equation (14) is often referred to in HCA literature as the uniform strain energy problem. The uniform strain energy problem formulation has been proven to yield optimal minimum compliance topologies by [18] and [17].

The HCA local update criteria for minimum compliance is given as

$$\bar{s}_{i_{k+1}} = \bar{s}_{i_k} + \Delta\bar{s}_i(k), \quad (15)$$

where the change in design variable $\Delta s_i(k)$ is given by

$$\Delta s_i(k) = f(e_{U_i}), \quad (16)$$

and e_{U_i} is the local strain energy error signal

$$e_{U_i} = U^* - \bar{U}_i(k), \quad (17)$$

where the subscripts i define the cellular automaton and the variable k define the algorithm iteration. The update function $f(U^* - \bar{U}_i(k))$ may take many forms depending upon control rule preference. For the purpose of this study, the proportional control method is adopted as the first choice. Equation 3 thus becomes

$$\Delta s_i(k) = C_f(-U^* + \bar{U}_i(k)), \quad (18)$$

where C_f is a constant or proportional control parameter. Special considerations are required in choosing an appropriate C_f and penalty factor p in Equation (1). Thorough investigations of the effect of control parameters and penalty factors were carried out in [17]. For the purpose of this investigation a penalty factor $p = 5$ was used to quickly drive the support structures to a zero one topology. Extensive investigations may be performed to select best the penalty factor for algorithmic stability and rapid convergence. Such work may be considered in future investigations.

In the simultaneous design of structural shape and supports, the HCA algorithm updates both \vec{s} and \vec{z} design domains during the update step of each iteration. As the support structure evolves, the deformation characteristics of the target plate are affected, changing the dynamic response of each node and the iterative shape update. The reverse effect also takes place. The simultaneous shape and support blast HCA algorithm developed in this investigation is depicted schematically in figure 5 and described as follows:

Step 1 Define the design domain from input finite element mesh and initial design $z(0)$.

Step 2 Conduct FEA numerical simulation.

Step 3 Evaluate the nodal response a_i, I_i from the LS-DYNA nodout FEA output file and collect spring energies U_i from elout FEA output file.

Step 4 Collect spring energies U_i from elout FEA output file.

Step 5 Calculate shape error signal e_i from Equation (9) and spring error signal e_{U_i} from Equation (17)

Step 6 Check for update conversion. If iteration update is within convergence criteria terminate updates; otherwise, apply update and continue with Step 2.

Dynamic deformation and support designs obtained from the simultaneous HCA method are presented in the following sections.

SIMULTANEOUS DESIGN RESULTS

The effect of impulsive constraints on the dynamic response and resultant stress distributions is evident from the numerical output of the baseline target structure generated in this investigation. Comparing the numerical output of the baseline design which includes an intermediate stiffness support domain with that of the unconstrained target, the difference in localized strain regions at the domain interface is clear. Stress profiles of a blast loaded plate of no shape depth and $\vec{s}(0)$ are depicted in figure 4.

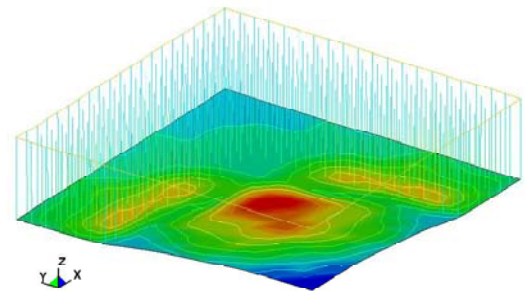


Figure 4: Fringe levels of one quarter of the initial design domain. Image produced by LS-PrePost of the stress levels in an impulsively constrained target plate subjected to a buried detonation.

From the fringe levels of stress output depicted in figure 4, the effect of impulse constraints caused by the support region and ballasted backing plate is evident near the artificially defined support boundaries. The impulse constraints imparted by the ballast generated out-of-plane deformations exhibited in the DRDC plate output that were not observed in unconstrained fluid

structure investigations. Stress and deformation patterns imparted by such ballasts are observed to be geometrically dependent. It is assumed that had the initial support design domain been defined differently, a different range of stress concentrations would have resulted.

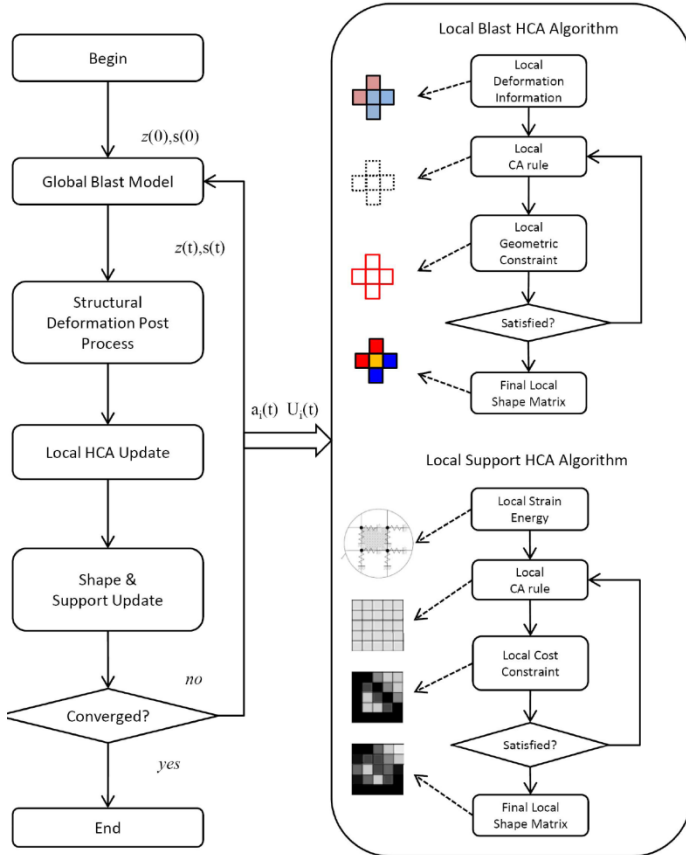


Figure 5: Schematic of the simultaneous HCA design algorithm for structure and supports

The simultaneous shape and support formulation will be evaluated for the loading conditions of a surface laid detonation and a shallow buried detonation. The baseline reaction to these two loading events is plotted in figures 6 and 7. The nodal displacement observed in these cases is caused by the ballast or impulsive constraints applied to the target structure.

Surface Laid Detonation

A surface laid blast is defined by the detonation of an explosive charge at an air media interface, where the media is representative of the ground with either a soil or sand material. The blast pressure exerted on the target in this case is usually greater than that of a free

field detonation due to the reflection of the blast from the ground interface. Such events are often approximated with empirical models, given certain assumptions of the reflection surface and blast proximity. From the MMALE formulation, we are able to simulate the blast event and record the blast profile exerted on the target in its entirety.

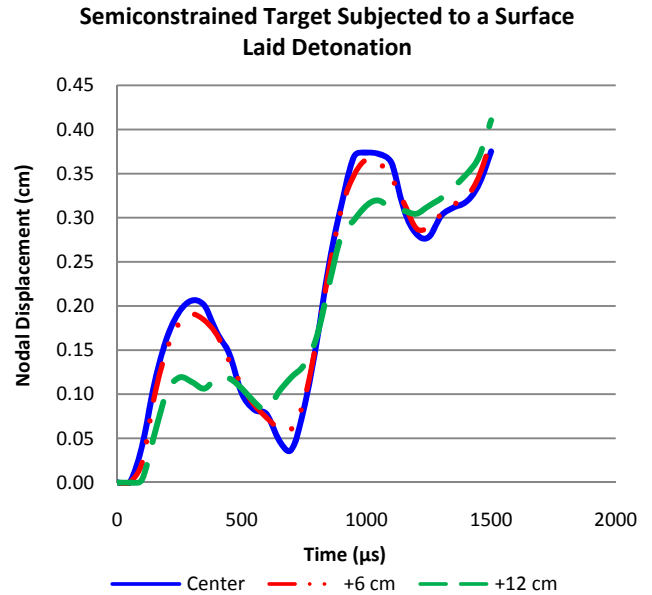


Figure 6: Baseline nodal displacements of a reference target plate subjected to a surface laid detonation.

Investigations of the fluid structure output from LS-DYNA's dbfsi output file are performed in order to record the blast pressure profile exerted on our design domain during this event. From these simulations we obtain the pressure profiles, peak pressure and pressure impulse results plotted in figures 8 and 10. In figure 8, we observe that there exists a difference in both the peak pressure and total impulse between the baseline target and the final design.

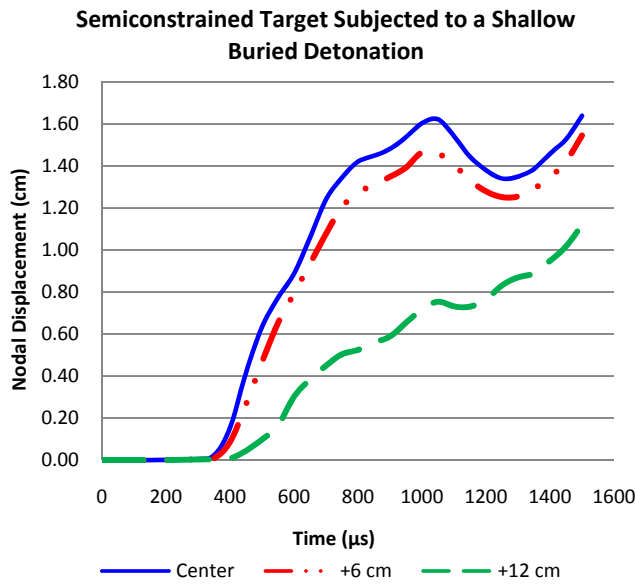


Figure 7: Baseline nodal displacements of a reference target plate subjected to a shallow buried detonation.

The characteristic single peak and exponential decay blast profile characterized by many free field detonation models is observed in the profile output. Since the proximity of the target is maintained throughout this investigation, we observe from figure 8 that the peak pressure occurs at the same time in both the initial and final target geometries. The reduction in peak pressure and impulse observed in figure 8 is more clearly depicted in figure 10. The peak pressure and blast impulse obtained is plotted by HCA algorithm iteration. We observe from figure 10 that the effect of the fluid structure interaction converges rather quickly: within the first 10 to 20 HCA algorithm iterations in this formulation.

The support location algorithm formulation meanwhile is updating the regions of highest stress with higher stiffness. The result of these updates is plotted in figure 9, where the regions of desired supports are depicted by areas of highest contours. As described in the algorithm formulation, these regions of high support density are arrived at by driving up the stiffness of highly stressed springs and driving down the stiffness of lesser stressed springs. The contours of highest density, depicted in figure 8, represent the remaining regions of highly stressed springs, and correspondingly highest demand for support locations.

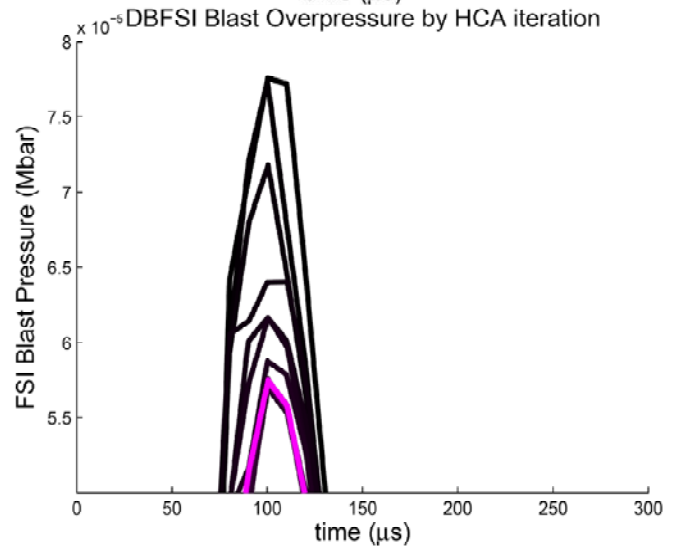
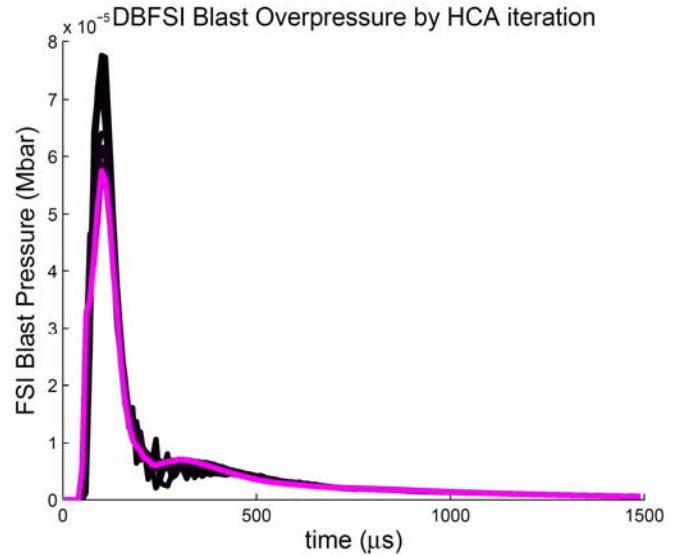


Figure 8: LS-DYNA FEA blast pressure output of a surface detonation by simultaneous shape and support by iteration. Iterations 1 to 20 are plotted from darkest to lightest.

It was observed that blast overpressure and impulse behaviors converge much more quickly than the nodal displacement output observed in this investigation. The simultaneous design schemes operate at different time scales, with the support design update lagging behind the shape design update. From figure 10, we see that the peak pressure reduction observed is on the order of 20% with a 10% reduction in blast impulse.

The degree of blast mitigation observed in this investigation is less than those observed in [3]. The cost of implementing ballast and geometric constraints on the fluid structure interaction problem is observed in

the difference between these pressure reduction studies.

The final topography design obtained from the HCA formulation is given in figure 14. The hull, assembly structure and support structure are depicted. A similar profile is observed for this case as that observed by Tan et al. in [3]. As was discussed and shown in figure 10, the final design yields significant blast overpressure and impulse reductions over the baseline. The mechanism by which these blast response reductions are achieved is often referred to by Hanssen et al. as the dishing or fluid structure interaction effect [2, 10].

Shallow Buried Detonation

A shallow buried blast is defined by the detonation of an explosive charge a few inches below the air soil interface. During the shock interaction phase of the blast event, the blast products form a deep conical depression in the soil. This depression is often referred to in literature as the debris cone. The debris cone serves to confine the blast wave, focusing the blast pressures in the regions directly above the center of the charge. Figure 11 depicts the pressure profiles exerted on the target by the shallow buried detonation event algorithm iteration.

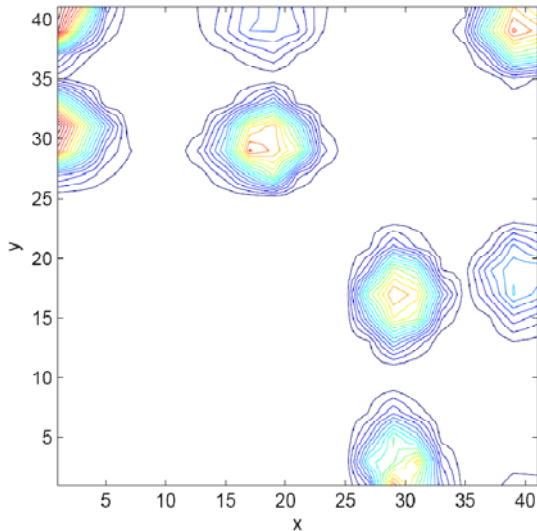
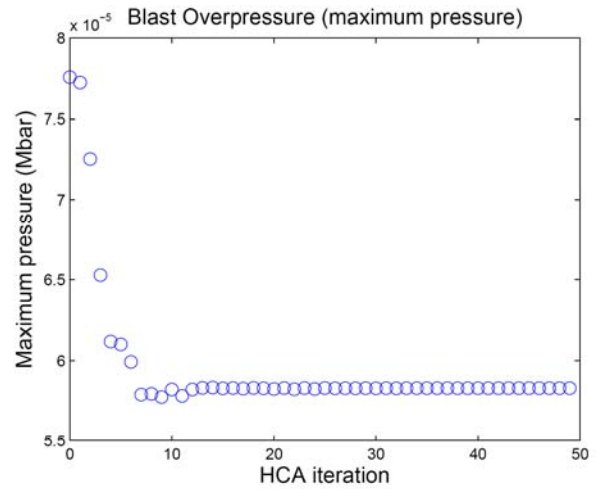


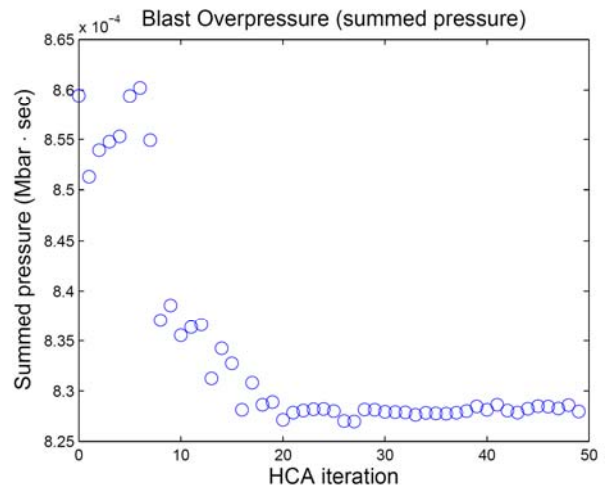
Figure 9: Design support regions by location obtained from HCA minimum compliance formulation for a surface detonation load case. One quarter of the overall target is depicted.

Comparing figure 8 to figure 11, we observe that the duration of the shallow buried blast pulse is much longer than the surface blast. Figure 12 depicts the reduction of shallow buried blast peak pressure and

impulse by HCA shape design. From figures 11 and 13 we observe that while the peak pressure of the shallow buried blast event is much lower than the surface blast event, the impulse of the shallow buried blast is much greater. This impulse magnification effect is due to the effect of soil confinement and the added ballast in extending the duration in which the target plate is held over the blast. Due to such confinement effects, such shallow buried detonation cases are commonly referred to as the most severe detonation scenario [13, 19].



(a) peak pressure



(b) summed pressure

Figure 10: Blast output from LS-DYNA FEA simulations of a surface detonation by simultaneous shape and support design iteration.

Simultaneous Topography Optimization of a Vehicle Hull and Topology Optimization of the Assembly Interface For Blast Mitigation, Tan, et al.

Desired support locations, as discussed for the surface detonation case, are similarly plotted for the shallow buried case in figure 12. It is observed that similar support regions are obtained in both detonation investigations. While nine support regions are highlighted in the surface detonation investigation, seven concentrated regions are obtained in the shallow buried blast event. The same target geometries, boundary conditions and CA algorithm parameters were applied to each case. The final support locations are shown here to be case dependent and highly coupled to the fluid structure solution.

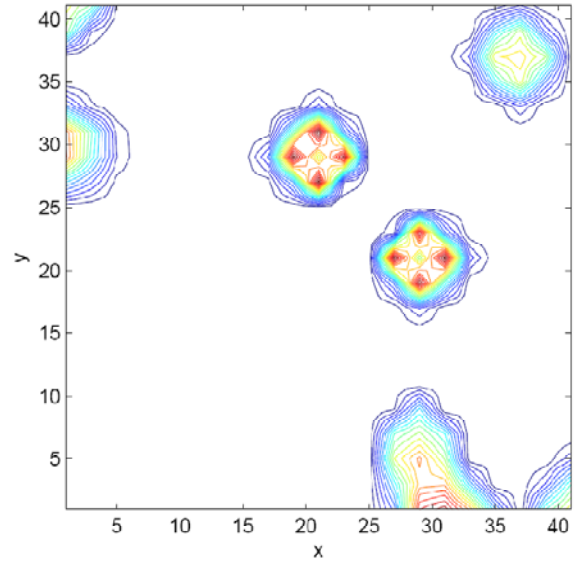


Figure 12: Design support regions by x and y location obtained from HCA minimum compliance formulation for a shallow buried detonation load case. One quarter of the overall target is depicted.

As similarly observed in the previous investigation, the peak pressure and blast impulses are reduced as the shape function is updated. A 25% reduction in peak pressure and 15% reduction in blast impulse are observed from the baseline design and the converged design. The physical coupling expected between the structural problem and fluid structure interaction problem is clearly evident and the simultaneous design of both domains is shown not only to be possible, but necessary.

The final shallow buried detonation design obtained from the HCA formulation is given in figure 15. The hull, assembly structure and support structure are depicted. Figure 13 depicts the reduction in blast pressure and impulse achieved by this final design over the baseline. As described by Hanssen et al. [2, 10], the fluid structure interaction characteristic is load dependant. The difference in load between the surface and shallow buried detonation cases is observable in the pressure profiles in figure 11 and the final design in figure 15.

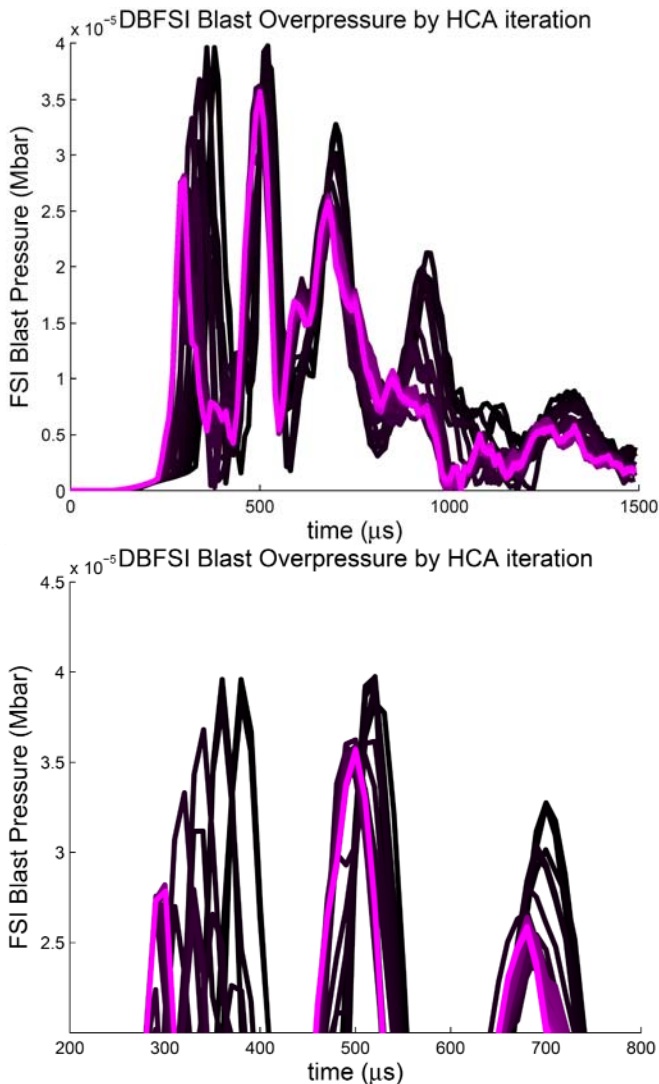
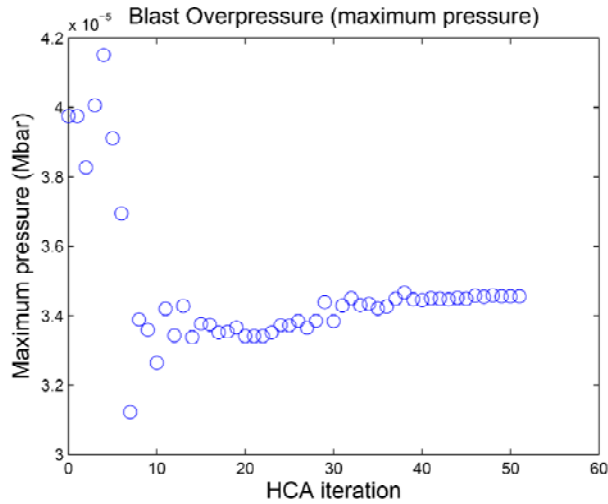
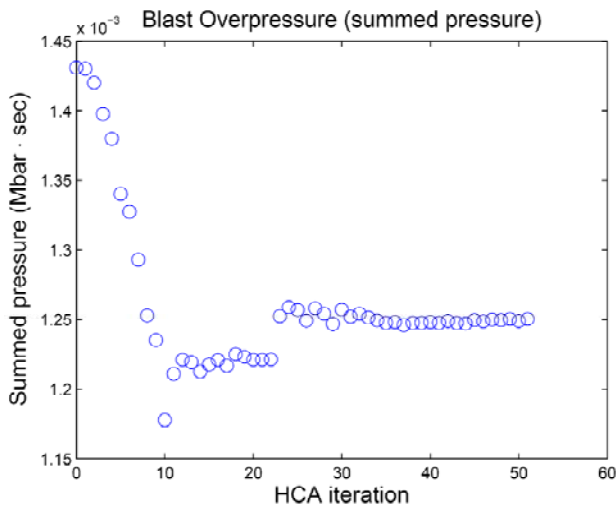


Figure 11: LS-DYNA FEA blast pressure output of a shallow buried detonation by simultaneous shape and support by iteration from darkest to lightest. Iterations 1 to 20 are plotted from darkest to lightest.

Simultaneous Topography Optimization of a Vehicle Hull and Topology Optimization of the Assembly Interface For Blast Mitigation, Tan, et al.



(a) peak pressure



(b) summed pressure

Figure 13: Blast output from LS-DYNA FEA simulations of a shallow buried detonation by simultaneous shape and support design iteration.

CONCLUSIONS

It has been shown from the investigations performed in this work that the discrete HCA scheme is capable of handling the simultaneous design of a fully coupled

fluid structure interaction with a simplified target. The design algorithm adopted in this methodology takes from both the node based topography optimization algorithm proposed by Tan et al. and the strain energy based topology optimization algorithm implemented in the original HCA formulation by Tovar et al. The effect of coupling these two methods simultaneously is observed in both the dynamic response of the target and the load on the coupled structure.

The effect of loading is observed to drive both the topography and topology designs of the target and support locations. From these findings, we observe the need to consider such loading conditions from a vehicle system design level as opposed to a component level. There exist many applications for which the HCA formulation offers algorithmic and design advantages. The high numerical demand and coupled nature of the blast mitigation problem makes this an ideal design problem for the HCA formulation.

The work presented thus far provides a proof of concept of ability to solve such coupled nonlinear dynamic problems. A proof of optimality is not available for the test problems evaluated and the global optimum of such problems are unknown. The double digit percentage reductions in blast loads resulting from such design rules is of great importance to the system and vehicle level design problems. In the vehicle level design problem, the exponential relation between blast impulse and the injury means that a 10% reduction in target acceleration has a dramatic effect toward reducing the ultimate design objectives of occupant injury metrics. Such reductions in occupant injury assessments are left for future investigations.

ACKNOWLEDGEMENTS

This material is based upon work supported by the U.S. Army TACOM Life Cycle Command under Contract No. W56HZV-08-C-0236 through a subcontract with Mississippi State University, and was performed for the Simulation Based Reliability and Safety (SimBRS) research program.

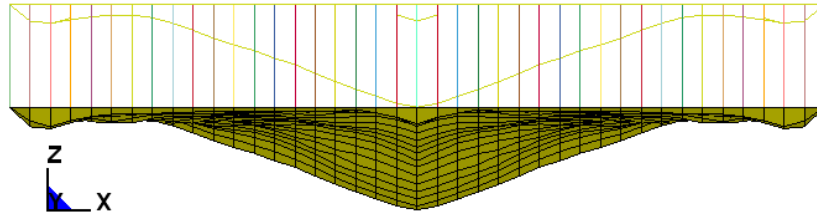


Figure 14: Final hull assembly design for the surface blast event. HCA topology convergence was observed after 10 algorithm iterations. The profile of the shaped hull is depicted with its corresponding support structure and backing plate.

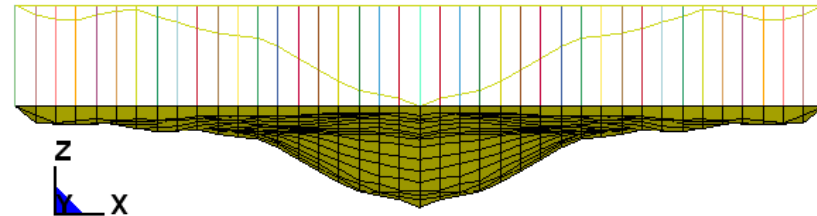


Figure 15: Final hull assembly design for the shallow buried blast event. HCA topology convergence was observed after 20 algorithm iterations. Notice the difference between the final topology between this design and that for the surface detonation event. Given the same CA neighborhood, error signal, penalty and finite element model, the dependence of the design on load condition is apparent

REFERENCES

- [1] "Occupant Crash Protection Handbook for Tactical Ground Vehicles," Department of Army, Washington, DC, 2000 .
- [2] Hanssen, A. G., 2002, "Close-Range Blast Loading of Aluminium Foam Panels," International Journal of Impact Engineering, 27(6) pp. 593.
- [3] Tan, H., Goetz, J., Tovar, A., 2010, "HCA Approach to Topography Design Optimization of a Structure for Fluid Structure Interaction," AIAA Structural Dynamics, and Materials Conference, AIAA, Fort Lauderdale, FL, .
- [4] Scott, B.R., 2006, "Lightweight Ballistic Composites; Military and Law-Enforcement Applications,"CRC Press, Cambridge, England, pp. 337-63.
- [5] Grujicic, M., Arakere, G., Bell, W. C. Haque, I., 2009, "Computational Investigation of the Effect of Up-Armouring on the Reduction in Occupant Injury Or Fatality in a Prototypical High-Mobility Multi-Purpose Wheeled Vehicle Subjected to Mine Blast," Proceedings of the Institution of Mechanical Engineers, Part D: Journal of Automobile Engineering, 223(7) pp. 903-920.
- [6] Buhl, T., 2002, "Simultaneous Topology Optimization of Structure and Supports," Structural and Multidisciplinary Optimization, 23(5) pp. 336.
- [7] Goetz, J., Tan, H., Tovar, A., 2009, "Topology Optimization of Aluminum Foam for Blast Mitigation Using Hybrid Cellular Automata," 2009 Ground Vehicle Systems Engineering and Technology Symposium, NDIA, Troy, MI, 1, .
- [8] Ma, , 2007, "Analysis of Foam Claddings for Blast Alleviation," International Journal of Impact Engineering, 34(1) pp. 60.
- [9] Guruprasad, , 2000, "Layered Sacrificial Claddings Under Blast Loading Part I—analytical Studies," International Journal of Impact Engineering, 24(9) pp. 957.
- [10] Børvik, T., Hanssen, A. G., Langseth, M., 2009, "Response of Structures to Planar Blast Loads – A Finite Element Engineering Approach," Computers & Structures, 87(9-10) pp. 507-520.
- [11] Pytleski, J. L. and Catherino, H., 1993, "Lightweight hull floor program," U. S. Army Research Laboratory, Watertown, MA, USA.
- [12] Condon J. A., Gniazdowski N., Gregory F. H., 1995, "The design, testing, and analysis of a proposed composite hull technology mine-blast-resistant vehicle floor panel," ARL-TR-796, .
- [13] Williams Kevin, M.S., 2003, "A Numerical Analysis of Mine Blast Effects on Simplified Target Geometries: Validation of Loading Models," Defence Research and Development Canada - Valcartier, Valcartier Canada.
- [14] Alia, A., and Souli, M., 2006, "High Explosive Simulation using Multi-Material Formulations," Applied Thermal Engineering, 26(10) pp. 1032-1042.

Simultaneous Topography Optimization of a Vehicle Hull and Topology Optimization of the Assembly Interface For Blast Mitigation, Tan, et al.

- [15] Krieg, R.D., 1972, "A Simple Constitutive Description for Cellular Concrete," Sandia National Laboratories, SC-DR-72-0883, Albuquerque, NM.
- [16] Neuberger, A., Peles, S., and Rittel, D., 2007, "Scaling the Response of Circular Plates Subjected to Large and Close-Range Spherical Explosions. Part II: Buried Charges," International Journal of Impact Engineering, 34(5) pp. 874-882.
- [17] Tovar, A., Patel, N. M., Niebur, G. L., 2006, "Topology Optimization using a Hybrid Cellular Automaton Method with Local Control Rules," 128(6) .
- [18] Tovar, A., Patel, N. M., Kaushik, A. K., 2007, "Optimality Conditions of the Hybrid Cellular Automata for Structural Optimization," 45(3).
- [19] Chafi, M. S., Karami, G., and Ziejewski, M., 2009, "Numerical Analysis of Blast-Induced Wave Propagation using FSI and ALEmulti-Material Formulations," International Journal of Impact Engineering, 36(10-11) pp. 1269-1275.

Simultaneous Topography Optimization of a Vehicle Hull and Topology Optimization of the Assembly Interface For Blast Mitigation, Tan, et al.

UNCLASSIFIED: Dist A. Approved for public release